



## Transactions of the IMF

The International Journal of Surface Engineering and Coatings

ISSN: (Print) (Online) Journal homepage: <https://www.tandfonline.com/loi/ytim20>

# Biomedical applications of polymer and ceramic coatings: a review of recent developments

J. R. Smith, D. A. Lamprou, C. Larson & S. J. Upson

To cite this article: J. R. Smith, D. A. Lamprou, C. Larson & S. J. Upson (2022) Biomedical applications of polymer and ceramic coatings: a review of recent developments, Transactions of the IMF, 100:1, 25-35, DOI: [10.1080/00202967.2021.2004744](https://doi.org/10.1080/00202967.2021.2004744)

To link to this article: <https://doi.org/10.1080/00202967.2021.2004744>



© 2021 The Author(s). Published by Informa UK Limited, trading as Taylor & Francis Group



Published online: 07 Dec 2021.



Submit your article to this journal [↗](#)



Article views: 355



View related articles [↗](#)



View Crossmark data [↗](#)

# Biomedical applications of polymer and ceramic coatings: a review of recent developments

J. R. Smith <sup>a</sup>, D. A. Lamprou <sup>b</sup>, C. Larson<sup>c</sup> and S. J. Upson <sup>d</sup>

<sup>a</sup>School of Pharmacy and Biomedical Sciences, University of Portsmouth, Portsmouth, UK; <sup>b</sup>School of Pharmacy, Queen's University Belfast, Belfast, UK; <sup>c</sup>Institute of Materials Finishing, Birmingham, UK; <sup>d</sup>Department of Life and Environmental Science, Bournemouth University, Bournemouth, UK

## ABSTRACT

Recent literature concerning the use of polymer and ceramic coatings for a variety of biomedical applications is surveyed in this review. Applications have been grouped into six broad categories: orthopaedic materials, cardiovascular stents, antibacterial surfaces, drug delivery, tissue engineering and biosensors. Polymer and ceramic coatings add enhanced corrosion protection, antiwear, antibacterial and biocompatibility properties to various substrates for biomedical applications. Processes favoured for polymer coating formation included dip, electrodeposition, spin (including electrospin) and spray (including electrospray and ultrasonic spray). Ceramic coatings were formed using magnetron sputtering and a combination of 3-D printing and *in-situ* mineralisation, among others. The review period is from 2017 to the present (mid-2021).

## ARTICLE HISTORY



Received 4 August 2021  
Accepted 29 October 2021

## KEYWORDS

Polymer coatings; conducting polymers; ceramics; orthopaedics; cardiovascular stents; antibacterial surfaces; drug delivery; tissue engineering

## List of abbreviations

β-TCP	β-tricalcium phosphate	NO	nitric oxide
AD-MSCs	adipose tissue-derived mesenchymal stem cells	NVP	N-vinylpyrrolidone
AMP	antimicrobial peptide	PCL	polycaprolactone
BCS	biolimus A9-coated stent	PDA	polydopamine
BMS	bare metal stent	PDE3	phosphodiesterase enzyme-3
BRS	bioresorbable stent	PDLCL	poly(D,L-lactic acid-co-caprolactone)
CAD	coronary artery disease	PDLLA	poly(D,L-lactic acid)
CCD	central composite design	PDMS	polydimethylsiloxane
CHX	chlorhexidine	PEDOT	poly(3,4-ethylenedioxythiophene)
CS	chitosan	PEG	polyethylene glycol
CS-BG	chitosan-bioactive glass	PEI	polyethyleneimine
CVD	cardiovascular disease	PGC-C18	poly(glycerol monostearate co-ε-caprolactone)
DAPT	dual antiplatelet therapy	PLA	polylactic acid
DCB	drug-coated balloons	PLCL	poly(L-lactide-co-caprolactone)
DEB	drug-eluting balloons	PLGA	poly(lactic-co-glycolic acid)
DES	drug-eluting stents	PLLA	poly(L-lactic acid)
DOX	doxorubicin	PMETA	poly(2-[(methacryloyloxy)ethyl] trimethyl ammonium chloride)
EC	ethyl cellulose	PNP	poly(N-methylpyrrole)
ECM	extracellular matrix	POPC	1-palmitoyl-2-oleoylphosphatidylcholine
EES	everolimus-eluting stent	PPy	polypyrrole
FDA	The US Food and Drug Administration	PQ	polyquaternium-10
GM	gentamicin	PSSG	poly(sorbitol sebacate glutamate)
GMA-MPA-N <sup>+</sup>	quaternary ammonium cations of maleopimaric acid	PU	polyurethane
GO	graphene oxide	PUC	polyurethane nanocomposite
GS	gentamicin sulphate	PVP	poly(vinyl pyrrolidone)
HAP	hydroxyapatite	RAFT	reversible addition-fragmentation chain-transfer
HPMC	hydroxypropyl methylcellulose	RSM	response surface methodology
ICPs	intrinsically conducting polymers	SA	sodium alginate
IEDDA	inverse electron demand Diels-Alder reaction	SCE	saturated calomel electrode
MCA	metal (copper)-catechol-(amine)	SES	sirolimus-eluting stent
MEA	microelectrode array	SIATRP	surface-initiated atom transfer radical polymerisation
MI	myocardial infarction	SMA	styrene maleic anhydride
MI-dPG	mussel-inspired dendritic polyglycerol	SRL	sirolimus
MNs	microneedle arrays	TA	tannic acid
MRSA	methicillin-resistant <i>S. aureus</i>	TNT	titanium nanotube
MSN	mesoporous silica nanoparticles	TROPO	tropoelastin
NiCHE	nature-inspired catechol-conjugated hyaluronic acid environment	VEGF	vascular endothelial growth factor
		ZES	zotarolimus-eluting stent

**CONTACT** J. R. Smith  james.smith@port.ac.uk  School of Pharmacy and Biomedical Sciences, University of Portsmouth, White Swan Road, Portsmouth PO1 2DT, UK

© 2021 The Author(s). Published by Informa UK Limited, trading as Taylor & Francis Group  
This is an Open Access article distributed under the terms of the Creative Commons Attribution-NonCommercial-NoDerivatives License (<http://creativecommons.org/licenses/by-nc-nd/4.0/>), which permits non-commercial re-use, distribution, and reproduction in any medium, provided the original work is properly cited, and is not altered, transformed, or built upon in any way.

## Introduction

Polymer and ceramic coatings for biomedical applications are areas of increasing interest.<sup>1</sup> Such coatings render their underlying substrate materials with biocompatibility, increased mechanical strength, wear resistance, corrosion resistance and functionality. The aim of this review is to bring up-to-date a previous review on the subject published in 2014.<sup>2</sup> In this paper, however, ceramic coatings in addition to polymer coatings are included. Ceramic coatings, especially in the biomedical area, are gaining ever increasing popularity.<sup>3</sup> Hydroxyapatite (HAP,  $\text{Ca}_{10}(\text{PO}_4)_6(\text{OH})_2$ ) is the obvious choice of ceramic material, due its similar composition to bone and biocompatibility, although it does have poor mechanical stability forbidding load-bearing use;<sup>4</sup> therefore, attempts have been made to improve this.

As in the 2014 review,<sup>2</sup> publications have been grouped into six main categories: orthopaedic materials,<sup>4–18</sup> cardiovascular stents,<sup>19–41</sup> antibacterial surfaces,<sup>42–56</sup> drug delivery,<sup>57–73</sup> tissue engineering,<sup>74–87</sup> and biosensors.<sup>88–95</sup> Each area is broadly structured from coatings on metallic to non-metallic surfaces. Papers featured in this review have been selected without application bias or emphasis from a larger pool of relevant studies to provide a spread of developments in the field to encourage the reader to want to explore further. The review period dates from 2017 to mid-2021.

## Applications

### Orthopaedic materials

Bacterial infection resulting from orthopaedic implants (osteomyelitis) is a leading cause of implant failure and revision surgery.<sup>5</sup> Chitosan (CS, a natural polysaccharide derived from crustaceans) combined with *Aloe vera* (CS/AV) loaded with gentamicin sulphate (GS) has been electrodeposited under potentiostatic conditions ( $-2.5$  V vs. SCE, 3-electrode system for 45 min) onto a Ti alloy. Increased antibacterial activity against *Staphylococcus aureus* (*S. aureus*) and *Escherichia coli* (*E. coli*) was found.<sup>5</sup> Chitosan-bioactive glass (CS-BG) nanocomposite coatings have been applied to Ti6Al4V using cathodic electrophoretic deposition by Mahlooji *et al.*<sup>6</sup> Increased BG content enhanced the apatite-forming ability of the coating, adhesion strength, roughness and wettability; good cell attachment and no significant levels of cytotoxicity were reported following this procedure. Mohan Raj *et al.* anodised Ti (at 50 V DC for 120 min in an electrolyte containing 3% sodium fluorosilicate), producing a  $\text{TiO}_2$ - $\text{SiO}_2$  surface onto which was subsequently electrodeposited ( $-2.5$  V vs. SCE for 45 min) a CS-lysine biopolymer coating and a final electrodeposited ( $-2.5$  V vs. SCE for 45 min) coating GS (50 mg  $\text{mL}^{-1}$  GS in the electrolyte), as a model drug.<sup>7</sup> The coating offered improved corrosion resistance and antimicrobial activity (*S. aureus* and *E. coli*) in addition to good osteoblast adhesion and growth. Kumari *et al.* carried out a systematic review on the use of CS-modified metallic and polymer scaffolds that are reported to enhance the biocompatibility, corrosion resistance and antibacterial properties of metallic implants.<sup>8</sup> Coating methods for CS using electrophoretic deposition, sol-gel methods, dip coating, spin coating or electrospinning are discussed.

Although Ti is used widely for implants owing to its excellent biocompatibility, the metal does suffer from insufficient

osteointegration that can affect implant longevity. Poly(*N*-methylpyrrole) (PNP) was electropolymerised on Ti using cyclic voltammetry (0.2 M *N*-methylpyrrole in 0.5 M sodium salicylate, 0.5–2.0 V vs. SCE, 10 cycles, 100  $\text{mV s}^{-1}$ ) followed by an electrodeposited layer of La-HAP (galvanostatic mode, 9  $\text{mA cm}^{-2}$ , 30 min).<sup>4</sup> This coating system led to decreased bacterial (*S. aureus* and *E. coli*) colonisation and increased microhardness, suggesting reduced likelihood for implant failure.<sup>4</sup> Introducing the rare metal lanthanum ( $\text{La}^{3+}$ ) into the HAP lattice increases the mechanical properties of HAP,<sup>9</sup> and acts as an antibacterial agent. The conducting polymer PNP, also has the potential for reducing inflammation and infection, and giving increased hardness and colonisation of the coating, compared to La-HAP alone.

Krishnakumar and Senthilvelan have reviewed the use of polymer composites in orthopaedic and dental applications over the past 10 years.<sup>10</sup> The review focused on polymers, some of which detail HAP/polymer composites replacing metals as bulk materials, however, rather than coatings *per se*.

Pan *et al.* examined zinc, cerium and selenium substituted HAP / poly (sorbitol sebacate glutamate) (PSSG) composite coatings on Ti (prepared by applying 50 V for 15 min at 27°C to Ti in 10 w/w% PSSG in HAP solution);<sup>11</sup> the metal ion substitution and the addition of PSSG were both found to increase microhardness. The composite coatings (containing  $\text{Zn}^{2+}$ ,  $\text{Ce}^{2+}$  and  $\text{SeO}_3^{2-}$ ) showed increased cell attachment, proliferation and differentiation to human osteoblasts MG-63 cells compared to similar composite coatings without these ions or with only single ion inclusion. Abdal-hay *et al.* coated Ti with a composite layer of magnesium particles and biodegradable polyurethane (PU) using spin-coating (Figure 1).<sup>12</sup> Superior corrosion resistance was found, although an alkaline-treatment step of the Ti prior to coating was important for enhanced adhesion. Cellular adhesion and proliferation was observed. The conducting polymer polypyrrole (PPy) has been electrodeposited, as a pectin/PPy composite loaded with gentamicin (GM), onto TiNbZr alloy.<sup>13</sup> Sustained release of GM was observed from the composite, and coatings with 10 wt% GM showed the lowest corrosion rate and highest biocompatibility and antibacterial performance.

Shokri *et al.* examined the pre-treatment and deposition of highly crystalline nano-Hap on to NiTi using the sol-gel spin coating technique.<sup>14</sup> A significant decrease in corrosion and  $\text{Ni}^{2+}$  release was found, and the materials showed enhanced biocompatibility.

Mendolia *et al.* coated AISI304 steel with brushite-hydroxyapatite/polyvinyl acetate using galvanic deposition (2 compartment cell; catholyte: 0.061 M  $\text{Ca}(\text{NO}_3)_2 \cdot 4\text{H}_2\text{O}$ , 0.036 M  $\text{NH}_4\text{H}_2\text{PO}_4$  and varying concentrations of vinyl acetate; anolyte: 1 M NaCl), different temperatures (25 and 50°C), deposition times (24 and 72 h) and different sacrificial anodes (zinc and aluminium, standard potentials of  $-0.762$  and  $-1.66$  V, respectively).<sup>15</sup> The best coatings were obtained using Al anodes. Cell viability assays showed that the coating enabled the stainless steel to support biocompatibility (MC3T3-E1 osteoblastic cells).

Samiee *et al.* formed a thin  $\text{TiO}_2$  layer and also a  $\text{TiO}_2/\text{MgO}$  double layer on AZ91D alloy (a magnesium die-cast alloy with excellent mechanical properties and corrosion resistance) using magnetic sputtering.<sup>16</sup>  $\text{TiO}_2$  and MgO phases were the main phases in the coatings (XRD examination), although in the double-layer coating,  $\text{MgTiO}_3$  and  $\text{Mg}_2\text{TiO}_4$  were

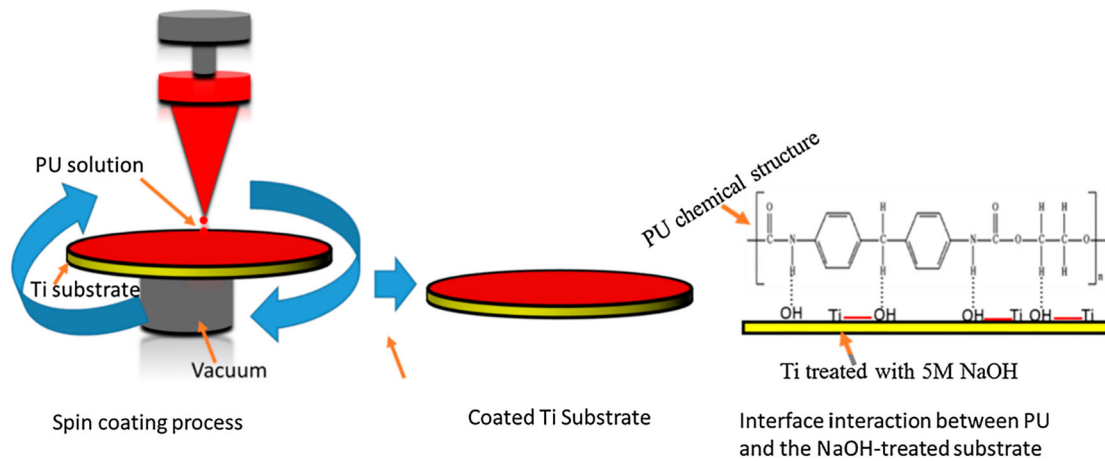


**Figure 1.** Spin-coating of Ti with PU showing electrostatic intermolecular interaction between the Ti and the polymer chain. Used with permission.<sup>6</sup>

additionally formed at the coating/substrate interface (Figure 2). The double layer coating showed the best corrosion resistance and enhanced biocompatibility and bio-adhesion was reported.

A dip-coating of polydopamine (PDA) containing chlorhexidine (CHX) applied to stainless steel was shown to prevent *Staphylococci* colonisation.<sup>17</sup> If the metal was dipped in PDA without CHX and then treated with CHX, however, this approach was found to compromise cell growth compared to the single dip method alone. PDA continues to be used as a coating for many types of surfaces; its use for orthopaedic implants has been reviewed by Jia *et al.*<sup>18</sup> The authors comment that PDA coatings provide a useful, cost-effective method for bestowing osteogenic properties and for subsequent modification using hydroxyapatite. Antibacterial properties can also be included by the addition of silver particles or other antimicrobial compounds (added during the process) to PDA coatings. The authors also state that a more detailed understanding of the interactions between cells and between PDA and extracellular matrix should be studied.

### Cardiovascular stents

Cardiovascular disease (CVD) claims 17.9 million lives every year, representing 31% of deaths globally.<sup>19</sup> Cardiovascular stents provide a treatment option from narrowed or blocked arteries, with the majority of stents being made of

either 316L stainless steel or cobalt-chromium (Co-Cr) due to their excellent mechanical properties and corrosion resistance.<sup>20</sup> Restenosis and thrombosis, however, can cause complications<sup>20</sup> and various coatings continue to be investigated.

Borhani *et al.*,<sup>21</sup> Beshchasna *et al.*,<sup>22</sup> Livingston and Tan,<sup>23</sup> and Lee and de la Torre Hernandez<sup>24</sup> have reviewed the innovative new advancements in the design and fabrication of cardiovascular stents. Borhani *et al.* have given particular focus on cardiovascular drug-eluting stents (DES), reviewing their design and development, as well as potential improvements of existing stents and a review on the fabrication of novel stent prototypes.<sup>21</sup> Beshchasna *et al.* also emphasise the mechanical aspects of stents and provide information on recently filed patents within the field.<sup>22</sup> Livingston and Tan<sup>23</sup> consider recent DES coating techniques and drug release profiles, while Lee and de la Torre Hernandez<sup>24</sup> provide suggestions regarding the optimal characteristics of future coronary stents.

Torii *et al.* reviewed stent designs, and their preclinical and pathology studies, focussing on neointimal coverage, thromboresistance and completeness of healing, concluding that further research is required to establish the relationship between modifications in stent design and improved outcomes.<sup>25</sup>

Rykowska *et al.* reviewed the design, materials and technologies used in the preparation of DES as well as drug-eluting balloons (DEBs).<sup>26</sup> With particular detail provided

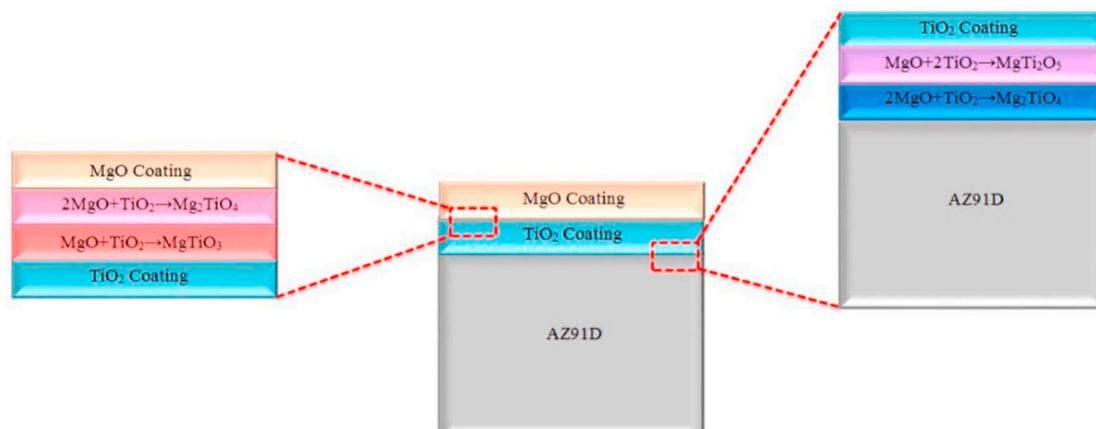


**Figure 2.** Cross-section showing composition of bilayer  $TiO_2$  and  $TiO_2/MgO$  coatings on AZ91D magnesium alloy for orthopaedic applications. Used with permission.<sup>16</sup>

into the most commonly used and researched polymers, this review concludes that although further research is required to achieve comparable efficacy and safety data, DES and DEBs present as significant alternatives for use in cardiac surgery.

Considering the current drawbacks thought to contribute to DES failure, Nojic *et al.*<sup>27</sup> have reviewed the clinical evidence supporting the use of biodegradable polymer and polymer free DES stents; Qiu and Zhao<sup>28</sup> reviewed the early stage development of bioresorbable stents (BRSs), taking into account both experimental and modelling work.

Krackhardt *et al.* conducted an unselected, single-armed, multicentre 'all corners' observational study enrolling participants from both Europe and Asia.<sup>29</sup> The clinical trial investigated the safety and efficacy of a polymer-free sirolimus (SRL, an immunosuppressant) coated, ultrathin strut DES concentrating on acute coronary syndrome. The study also considered stable coronary artery disease (CAD) with dual antiplatelet therapy (DAPT) over short, ( $\leq 6$  months) vs. long ( $> 6$  months) time periods. The authors concluded PF-SES angioplasty to be safe and effective and that DAPT duration of over 6 months did not have lower target lesion revascularisation rates in comparison to those with durations of up to 6 months, indicating that in patients with stable CAD, extended DAPT duration past 6 months did not improve clinical outcomes.

Noting the potential of stents that can inhibit restenosis without adversely affecting re-endothelialisation, McKittrick *et al.* optimised an electrospray deposition process, producing a series of rapid release accelerate™ AT-sirolimus coatings offering similar release kinetics, drug load and coating thickness to DES used clinically.<sup>30</sup> The coatings also demonstrated bioactive properties, by stimulating attachment of primary porcine endothelial cells.

Jeger *et al.* identified that clinical outcome data related to the use of DEBs (also known as drug-coated balloons, DCBs) beyond one year is needed. They also conducted a long-term follow-up of a multicentre, randomised, open-label, non-inferiority trial (2012–2017).<sup>31</sup> The study examined paclitaxel-coated DCBs, and everolimus- and paclitaxel-eluting DES. The trial results indicated that in the use of DCBs (vs. DES) in the treatment of *de novo* coronary artery small vessel disease, efficacy and safety were maintained for up to 3 years.

Bakola *et al.* fabricated a drug delivery nano-system consisting of electrospun hydrophobic polylactic acid (PLA) fibrous scaffold loaded with dipyridamole (a nucleoside transport inhibitor and a phosphodiesterase enzyme-3 (PDE3) inhibitor), added during the electrospinning process.<sup>32</sup> The surface morphology and topography were found to be suitable for tissue engineering, and further studies revealed that the fibrous nanoplateforms enhance cytocompatibility when used with mice fibroblasts (L929) and are capable of sustaining a controlled release of dipyridamole.

Bae *et al.* fabricated a peptide-coated stent WKYMMm (Trp-Lys-Tyr-Met-Val-D-Met) utilising a peptide specifically synthesised to stimulate endothelial cell proliferation;<sup>33</sup> this was achieved by essentially dip-coating a Co-Cr bare metal stent (BMS) in dopamine followed by a solution containing peptides. Results from mechanical testing, endothelial cell proliferation and pre-clinical animal studies demonstrated that the peptide-coated stent was not inferior to the drug-eluting scaffolds tested for comparison. The authors also suggest a secondary coating with immunosuppressive

drugs, such as everolimus and biolimus, could also be incorporated.

Utilising an ultrasonic spray technique, Roopmani *et al.* coated a bare metal stent with a drug loaded (atorvastatin and fenofibrate) biodegradable polyester poly(L-lactide-co-caprolactone) (PLCL) coating.<sup>34</sup> The coating was found to be uniform, defect free and biocompatible (Wistar rat study), anti-inflammatory and antithrombotic properties were also exhibited.

Navarro *et al.* investigated the reasons behind the clinical failure of gold and carbon-coated 316L stainless steel stents (Inflow Gold Flex System, Inflow Dynamics, and Carbon film™ Coated Coronary Stent, Sorin, Biomedical, respectively); many of these systems were approved and put into service globally, although had to be withdrawn due to high levels of failures, with little understanding of the mechanism.<sup>20</sup> The Au and C coatings were found to result in pitting corrosion of the underlying 316L substrate, leading to a release of toxic ions. In addition, the high restenosis rate of Au coated 316L stents was attributed to a synergistic effect of Au ions with the ions from the pitting corrosion event. The authors propose complementary techniques that can be used alongside the FDA guidance during early non-clinical engineering tests.

Realising the need for improved degradability in biocompatible phosphorylcholine based polymer coatings, Liu *et al.* presented a method to synthesise a biodegradable phosphorylcholine copolymer utilised to form a stable coating, on hydrophobically silanised glass, *via* ultrasonic spraying.<sup>35</sup> The synthesised copolymer coatings exhibited biocompatibility, anti-adhesion properties and a sustained release profile of rapamycin (also known as SRL).

To address the current problems associated with in-stent stenosis, Yang *et al.* presented a step-wise method utilising a metal (copper)-catechol-(amine) (MCA) strategy;  $\text{Cu}^{2+}$ , catechol and a diamine form a complex on the surface of a 316L stainless steel when dipped into the solution.<sup>36</sup> This surface was then coated with heparin (carbodiimide chemistry) and a nitric oxide (NO)-releasing coating to produce a multifunctional endothelium-mimicking surface, that controllably released these compounds.<sup>36</sup> Li *et al.* also recognised the benefits of NO (a signalling molecule in vascular biology) in CVD and developed an NO-generating coating ( $\text{Cu}^{2+}$ -Dopa) (dip-coating, 24 h) utilising a metal-catecholamine framework, which promoted re-endothelialisation, suppressed thrombosis and showed a reduction in intimal hyperplasia (accumulation of cells) *in vivo*.<sup>37</sup>

In an effort to enhance the corrosion resistance of bioresorbable magnesium alloy (WE43) stents, Lakalayeh *et al.* investigated the use of FDA approved polymers, PLA, polycaprolactone (PCL) and poly(lactic-co-glycolic acid) (PLGA) applied as dip-coatings.<sup>38</sup> Both PLA and PLGA exhibited corrosion resistance, with PLA also demonstrating biocompatibility.

Also, noting the need for enhanced corrosion resistance, Xu *et al.* dip-coated Mg alloy (AZ31) stents with silk fibroin, followed by an ultrasonic spray coating of PDLLA and PCL containing SRL;<sup>39</sup> release of SRL was demonstrated, with ethanol treatment of the coated stent shown to slow the release of the drug. Biocompatibility was established utilising human umbilical vein endothelial cells and minimal platelet adhesion; the coated stent also exhibited uniform corrosion, a property thought to be advantageous in maintaining the

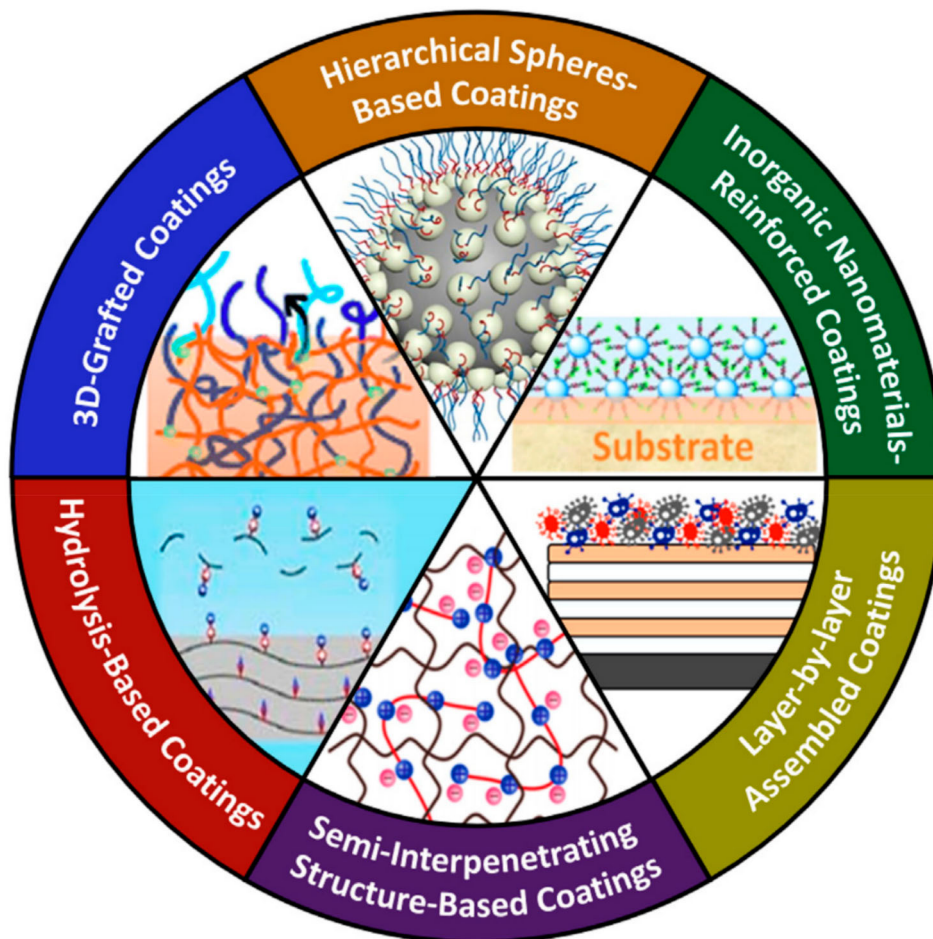


**Figure 3.** Strategies to prepare mechanically and chemically durable hydrophilic polymer-based coatings. Used with permission.<sup>42</sup>

stent's radial strength. The same authors also performed an earlier similar study, using similar polymers without the silk fibroin addition.<sup>40</sup>

To increase the growth of endothelial cells on Mg–Zn–Y–Nd alloy surface and promote the wider use of magnesium alloys, Chen *et al.* immobilised (6 h immersion) a specific link peptide of endothelial cells, Arg–Glu–Asp–Val (REDV), onto a PDA-deposited (24 h immersion) Mg–Zn–Y–Nd alloy surface.<sup>41</sup> The obtained coating exhibited anti-hyperplasia and anti-inflammatory properties.

#### Antimicrobial surfaces

Huang and Ghasemi have reviewed mechanically and chemically robust anti-biofouling hydrophilic polymer coatings;<sup>42</sup> these were classified into six types: (i) 3D-grafted coatings, (ii) hierarchical spheres-based coatings, (iii) inorganic nanomaterials-reinforced coatings, (iv) hydrolysis-based coating, (v) semi-interpenetrating structure-based coatings, and (vi) layer-by-layer (LbL) assembled coatings (Figure 3).

The antibacterial coating polyterphenol has been plasma polymerised on four types of Ti surfaces, each with different micro- and nano-scale topographies;<sup>43</sup> the antimicrobial (*E. coli* and *Pseudomonas aeruginosa*) action was significantly enhanced with polymers plasma-coated on Ti with lower degrees of nanoscale roughness, *i.e.* after mechanical and chemical polishing. Valliammai *et al.* produced polymer coatings containing citral and thymol as active ingredients on Ti using spin coating;<sup>44</sup> sustained release was noted for 60 days and the coating effectively inhibited methicillin-resistant *S. aureus* (MRSA), whilst being hemocompatible.

In an effort to protect Ti with a simple and convenient anti-bacterial/antifouling coating, Guo *et al.* investigated coatings of tannic acid (TA) and polyethylene glycols (PEGs);<sup>45</sup> the Ti-TA/PEG surface, formed from deposition (dip coating) from a mixture of TA and PEG, rather than sequential dipping, produced a thicker coating that minimised bacterial adhesion, prevented biofilm formation and reduced platelet adhesion.

Liu *et al.* capitalised on the strong covalent binding ability of phosphonate groups to Ti to link cationic quaternary ammonium polymers to Ti *via* metal-anchorable phosphonate motifs;<sup>46</sup> excellent antibacterial properties were reported.

Realising that most implant antimicrobial coatings are fixed and predetermined prior to implantation, Czuban *et al.* developed an alternative strategy.<sup>47</sup> Ti was coated, using a dip-coating procedure, with mussel-inspired dendritic polyglycerol (MI-dPG) that could be locally activated with a prodrug (daptomycin) to treat MRSA (Figure 4).

Dhingra *et al.* developed a polymer brush layer, *via* surface initiated atom transfer radical polymerisation (SIATRP), onto tartaric acid-based hydroxyl functionalised biodegradable aliphatic polyester (on glass), that displayed an optimal performance of antimicrobial action and biocompatibility;<sup>48</sup> there is a known trade-off between these properties.<sup>49</sup> The optimal polymer brush consisted of poly(2-[(methacryloyloxy)ethyl] trimethyl ammonium chloride) (PMETA) brush and was formed after 18 h (to establish a 400 nm optimum brush length), exhibiting the highest antibacterial activity (> 97% and > 96% killing efficiency for *E. coli* and *S. aureus*, respectively) and reasonable cytocompatibility (> 70%).

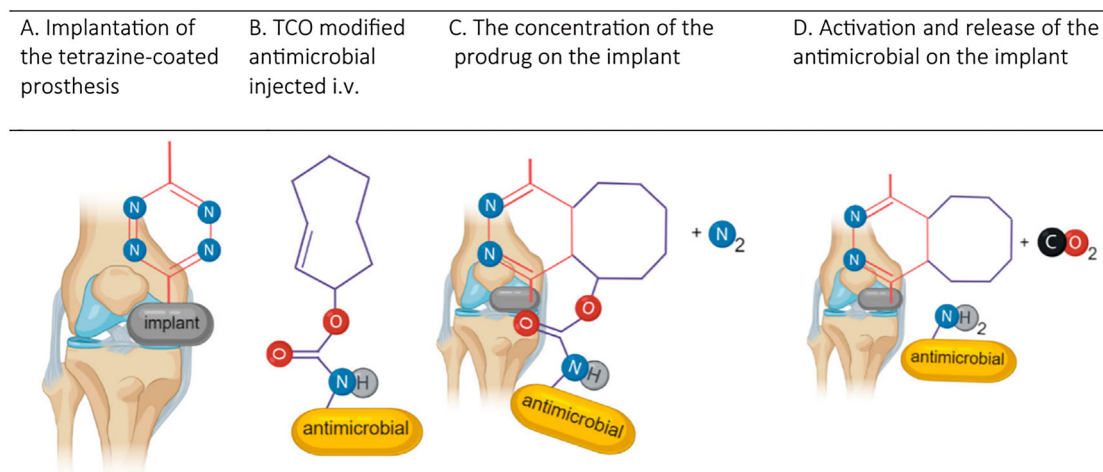


**Figure 4.** Concept of inverse electron demand Diels-Alder reaction (IEDDA)-based titanium antimicrobial coating that concentrates, activates, and releases intravenously injected prodrug antimicrobial: (A) The tetrazine-coated prosthesis is implanted in the infected area, (B) caged prodrug added systemically, (C) prodrug covalently reacts with the coated implant, and (D) IEDDA reaction uncages the prodrug, forming an active drug. Used with permission.<sup>47</sup>

Wang *et al.* have developed a multifunctional (UV-absorbing, self-healing, antibacterial, water-stable, glass-adhesive, and abrasion-resistant) protective film for touch-screen panels, utilising a novel nano-antimicrobial agent involving polyquaternium-10 (PQ) and sodium alginate (SA) with TiO<sub>2</sub> nanoparticles (PQ-TiO<sub>2</sub>-SA);<sup>50</sup> aSA-PQ microgel solution was cast on to glass followed by cross-linking with peroxy titanate and *in situ* formation of TiO<sub>2</sub> nanoparticles through hydrolysis of the peroxy titanate. Quercetin and resveratrol nanoparticles were also incorporated to produce a coating effective against *S. aureus* and *E. coli*.

Li *et al.* produced an antimicrobial graft polymer coating of *N*-vinylpyrrolidone (NVP) and quaternary ammonium cations of maleopimaric acid (GMA-MPA-N<sup>+</sup>), *via* surface-initiated reversible addition-fragmentation chain-transfer polymerisation, on polydimethylsiloxane (PDMS) silicone elastomer (Figure 5);<sup>51</sup> the coating showed biofilm inhibition to Gram positive (*S. aureus*) and Gram negative (*E. coli* and *P. aeruginosa*) bacteria for 21 days and significant platelet adhesion, whilst maintaining biocompatibility. Low *et al.* dip-coated silanised silicone (PDMS) in a solution of PCL, PEG and antimicrobial peptide (AMP, an in-house synthetic polypeptide), followed by a solution of ethyl cellulose (EC): 1-palmitoyl-2-oleoylphosphatidylcholine (POPC);<sup>52</sup> the coating was successful in targeting planktonic bacteria and biofilm formation in urinary catheters. Sustained release was achieved, and antibacterial (*S. aureus*, *E. coli* and *P. aeruginosa*) activity was noted for over 6 days.

Hung *et al.* treated polypropylene with UV-ozone, to expose carboxylic acid groups that were then converted to anhydride groups to enable coupling of branched polyethyleneimine (PEI) containing various molecular mass styrene maleic anhydride (SMA) crosslinkers;<sup>53</sup> the coatings were investigated in their inherent, cationic form, and as their chlorinated derivatives. The best antimicrobial effect against *E. coli* was with 6 kDa SMA and the coating was chlorinated (and more stable).

Su *et al.* coated textile fabrics consisting of cotton, wool, and polyethylene terephthalate with poly(catechol) and poly(*p*-phenylenediamine) *via in situ* enzymatic polymerisation of these monomers;<sup>54</sup> antimicrobial activity against *S. aureus* and *E. coli* was demonstrated.

Ahmadi and Ahmad developed an anti-corrosion and antimicrobial polyurethane nanocomposite (PUC) containing

graphene oxide (GO), pongamia oil and acrylic acid (to induce  $\pi$ - $\pi$  interactions) that was applied to carbon steel using a brush technique;<sup>55</sup> GO additions of 0.5%wt increased the anti-corrosion behaviour of the PUC (increased corrosion potential and impedance modulus at low frequency; decreased corrosion current density) even after 21 days and was effective against *S. aureus* and *E. coli*.

Nguyen *et al.* reported that the topography of surfaces and coatings can be tailored to reduce microbial attachment;<sup>56</sup> self-organised wrinkles show particular promise (Figure 6).

#### Drug delivery

An historical perspective on the use of drug delivery systems (e.g. nanoparticles, liposomes, hydrogels, cationic-and emulsion-based carriers) for use with osteoarthritis and rheumatoid arthritis patients has been presented by Saeedi *et al.*<sup>57</sup> Advantages and disadvantages of the carrier systems are discussed, as are factors affecting delivery, such as charge, size, structure and release rates. Jana *et al.* also provide a review of drug delivery systems, some of which involve polymeric coatings.<sup>58</sup>

$\beta$ -Tricalcium phosphate ( $\beta$ -TCP) bioceramic is a resorbable bone graft, although drug delivery from this material is too fast due to its microporosity.<sup>59</sup> Khurana *et al.* used plasma polymerisation (monomer: diethylene glycol dimethyl ether) to produce PEG-like coatings (10–40 nm) on  $\beta$ -TCP loaded with antibiotics (ampicillin and GS).<sup>59</sup> The antimicrobial effect (*S. aureus*) was unaffected and the surfaces remained cytocompatible (human osteosarcoma cells).

Yu *et al.* produced a drug-eluting polymer film by dip-coating a silicone electrode array of a cochlear implant into a precursor solution of poly lactic-co-glycolic acid (PLGA) and trichloromethane containing one of three drugs (dexamethasone sodium phosphate, cytosine arabinoside hydrochloride or nicotinamide adenine dinucleotide).<sup>60</sup> The drugs were released in a sustained manner, showing promise for reduced risk of intra-cochlear infection. Sevostyanov *et al.* pulled metal stent wires through a solution of PLGA containing streptokinase, which is an enzyme with high thrombolytic activity, followed by controlled evaporation steps.<sup>61</sup> The enzymes retained *ca.* 90% of their activity in the resultant coating and were released in a controlled manner; no short-term toxic effects on cells were shown by the polymer coating.

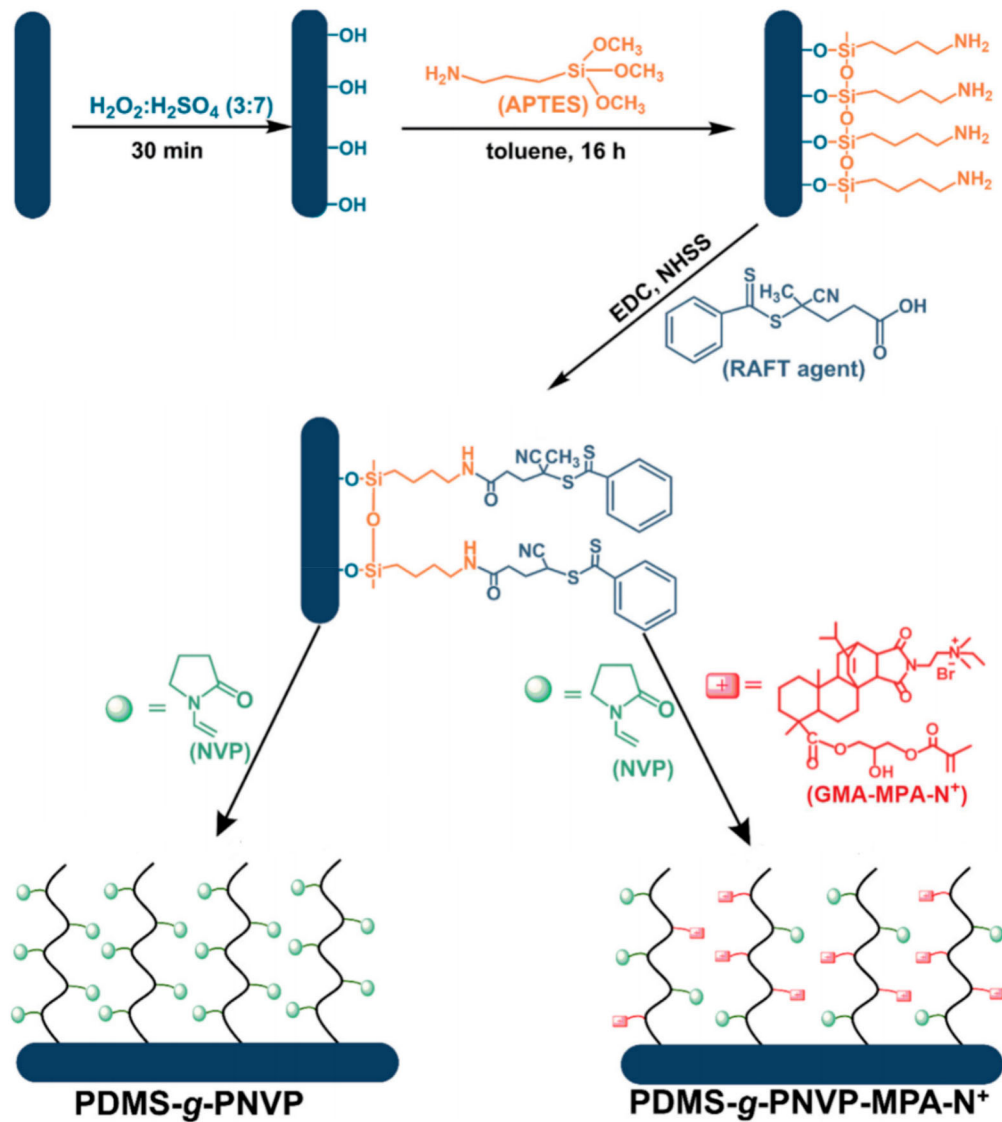


**Figure 5.** Preparation of dual-function antimicrobial coating using NVP and GMA-MPA-N<sup>+</sup> via the reversible addition-fragmentation chain-transfer (RAFT) reaction. Used with permission.<sup>51</sup>

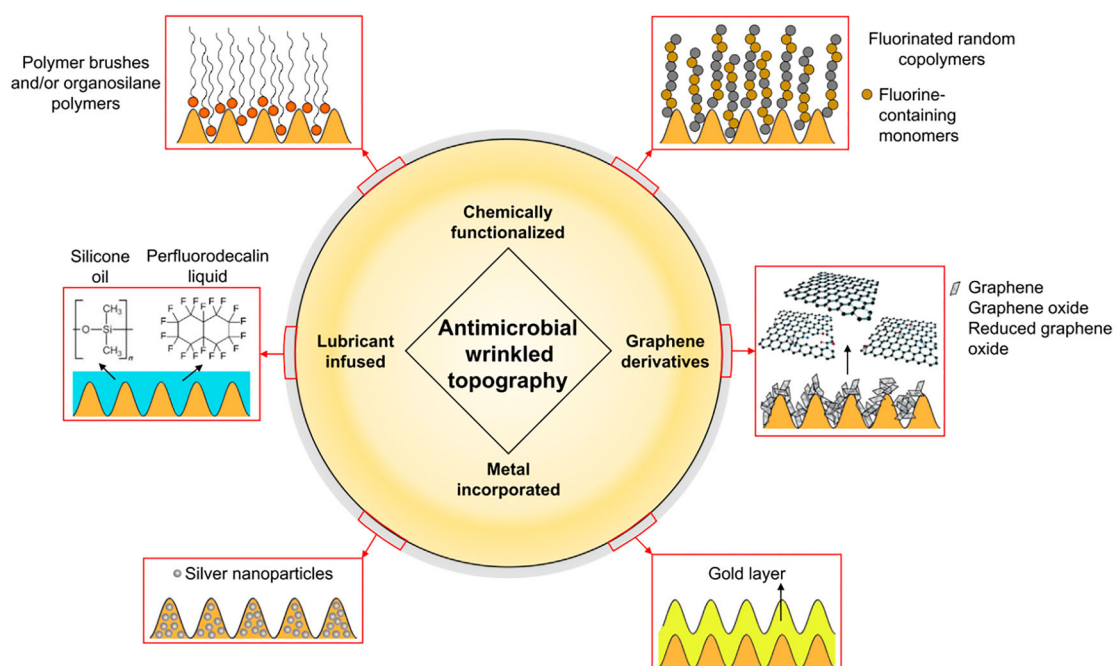


**Figure 6.** Emerging antimicrobial wrinkled topographies can be categorised in four areas: chemically functionalised, graphene derivatised, metal incorporated, and lubricant infused. Used with permission.<sup>56</sup>



Al Subeh *et al.* coated fibrous meshes of polyglycolic acid (PGA), formed by electrospinning, with poly(glycerol monostearate co- $\epsilon$ -caprolactone) (PGC-C18) containing a novel anticancer drug eupenifeldin, using a layer-by-layer technique;<sup>62</sup> the coatings were introduced *via* a syringe and time allowed for solvent (dichloromethane) evaporation between layering. These buttresses were intended for use as implants along the surgical margin following lung cancer tumour resection. Prolonged drug release approaching 90 days was observed *in vitro*.

Response surface methodology (RSM) based on a central composite design (CCD) was used by Moghimipour *et al.* to evaluate the combination of pH and time-dependent release of theophylline from gelatin capsules dip-coated in hydroxypropyl methylcellulose (HPMC) and Eudragit® FS 30 D.<sup>63</sup> Results indicated that the designed system could be used as a carrier for colon drug delivery.

Barakh Ali *et al.* coated core tablets using an 8" Vector Hi-Coater (with various inlet temperatures, bed temperatures, pan rotation speeds, atomisation pressures and spray rates) to 5 and 10% w/w mass gain with different polymer blends to increase or prolong their dissolution and release of the model drugs diclofenac sodium and prednisone;<sup>64</sup> blends of cellulose ester and enteric polymers were investigated.

A spray comprising the natural biopolymer pectin (a bioadhesive hydrogel) and drug nanocrystals coated with polylactic acid-polyethylene glycol (NCPPs) was proposed for use in treatment of glioblastoma (malignant brain tumour).<sup>65</sup> The coating, stabilised with Pluronic F127, would be sprayed on resected brain tissue; etoposide and olaparib NCPPs at high drug loading showed *in vitro* stability and drug release over 120 h.

Microneedle arrays (MNs) are a method of introducing drugs across the skin overcoming the obvious disadvantages of conventional hypodermic needles.<sup>66</sup> A review on polymeric MNs has been published by Singh *et al.*<sup>67</sup> Examples of drugs used in MNs, include the influenza vaccine, lidocaine, insulin, miconazole and 5-fluorouracil.<sup>68</sup> Cárcamo-Martínez *et al.* made MNs by pouring a Gantrez®S-97 (a copolymer of methylvinylether and maleic acid (molecular mass 1,500 kDa) / PEG200 mixture) on a silicone mould.<sup>68</sup> The MNs were then coated (10  $\mu$ L drop and left to dry) with a model drug, 2 w/w% rhodamine B (in 20% PVP and 99.5% ethanol, with different amounts of glycerol and Tween® 80), to test their efficacy. Polymer MNs have the advantage of improved biocompatibility, reduced fracture probability and reduced likelihood of leaving fragments on the skin compared with silicon, glass and ceramics MNs.

Xu *et al.* produced a curcumin polymer shell coating on mesoporous silica nanoparticles (MSNs), using silane and thiol coupling chemistry, for use in cancer treatment.<sup>69</sup> The polymer shell had three functions: (1) to gate MSN pores and retained doxorubicin (DOX) within pores; (2) to degrade and release curcumin (also an anticancer drug); and (3) aid fluorescence imaging as curcumin is self-fluorescent.

Deposition of CS on the surface of titanium nanotube (TNT) arrays using a dip-coating process for the controlled release of drugs was reported by Shidfar *et al.*; CS coating thicknesses of 0, 0.29 and 0.45  $\mu$ m achieved drug (gentamicin) release times for about 6, 8 and 12 days, respectively.<sup>70</sup>

Peng *et al.* coated Fe<sub>3</sub>O<sub>4</sub> nanoparticles with zwitterionic polymer membranes, *via* silane chemistry, to improve the stability of the nanoparticles, which is important in drug

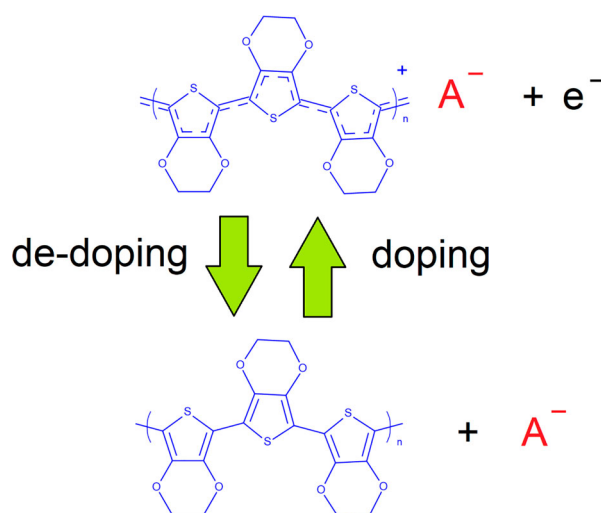


**Figure 7.** Reversible redox activity of a conducting polymer between doped (oxidised) and de-doped (reduced) states. Poly(3,4-ethylenedioxythiophene) (PEDOT) is shown in the example.

delivery for treating cancer, where long blood circulation is required.<sup>71</sup>

Intrinsically conducting polymers (ICPs) use as drug delivery systems was recently reviewed by Puiggali-Jou *et al.*<sup>72</sup> The review pays particular attention to drug release following electrical stimuli, where charged drug molecules can be expelled from the charged polymer matrix (Figure 7).

Electrochemical methods are also used to deposit ICPS onto conducting substrates. Examples of drugs incorporated in the review include: *N*-methylphenothiazine, phenothiazine, quercetin, ciprofloxacin, neurotrophin-3, chlorpromazine, brain-derived neurotrophic factor, risperidone, acetylcholine chloride, dopamine hydrobromide, ibuprofen (anionic form), methotrexate, heparin, ATP and betulin.

Although the use of conducting polymers and hydrogels for drug release is not new, the combination of these materials is an emerging area. Bansal *et al.* have reviewed the use of conducting polymer hydrogels for such applications.<sup>73</sup> Particular advantages include biocompatibility, improved mechanical properties, increased drug loading and ability to deliver hydrophilic drugs, although there are only a few *in vivo* examples currently.

### Tissue engineering

In an effort to mimic both the organic and inorganic phases of bone extracellular matrix (ECM), Caddeo *et al.* utilised surface silanisation with a successive chemical grafting technique to coat slices of bioactive glass ceramic (representing the inorganic phase of bone) with a type I collagen PU blend (representing the organic phase of bone).<sup>74</sup> Results showed the successful synthesis of a water soluble PU assessed as non-toxic (MG-63 osteoblast-like cells), the collagen-PU coating also demonstrated biocompatibility (human periosteal derived precursor cells) with an increased deposition of mineral matrix, suggesting the coated substrate has potential for bone cell adhesion and growth.

Kiran *et al.* fabricated hybrid PCL/TiO<sub>2</sub> coatings on commercially pure Ti substrates, utilising electrospinning to fabricate coatings with varying concentrations of TiO<sub>2</sub> nanoparticles.<sup>75</sup> The obtained nanocomposite scaffolds exhibited bioactivity and improved biocompatibility when compared with uncoated and PCL-coated substrates as well

as antimicrobial activity (*S. aureus*), thought to be of use in preventing potential infections.

Considering their ability to allow for autologous recellularisation, preservation of native vessel architecture and eliminating cell-based antigens, decellularised vascular grafts have recently been investigated within the field of tissue engineering for their potential use in cardiac medicine.<sup>76,77</sup> To reduce the risk of thrombosis and degeneration, Marinval *et al.*<sup>76</sup> and Iijima *et al.*<sup>77</sup> have engineered coatings on decellularised vascular grafts. To improve the re-endothelialisation and reduce the thrombogenicity and calcification of decellularised porcine heart valves, Marinval *et al.* manually coated a valve scaffold with 3 layers of a fucoidan / vascular endothelial growth factor (VEGF) polyelectrolyte multilayer film (PEM).<sup>76</sup> The coating demonstrated the desired gain in antithrombotic activity without increasing calcification. The modified scaffold also exhibited enhanced re-endothelialisation and improved potential for stem cells repopulation. Iijima *et al.* coated the internal surfaces of aortic grafts (Wistar rats) with a hydrogel-VEGF mixture by quickly warming to 37°C to polymerise the coating as a gel inside the lumen.<sup>77</sup> *In vivo* results showed the coating stimulated medial recellularisation and significantly increased endothelium formation in comparison to the uncoated graft control group.

Cardiac remodelling is a common consequence of myocardial infarction; recently, stem cell-based therapy has been garnering attention as a potential approach to regenerate cardiac tissue and prevent the formation of non-contractile scar tissue. Chen *et al.* utilised electrospinning and layer-by-layer coating technology to produce a cardiac patch-based system utilising CS/silk fibroin, which was further engineered to engraft adipose tissue-derived mesenchymal stem cells (AD-MSCs).<sup>78</sup> *In vivo* studies revealed the CS/silk fibroin nanofibrous patches improved both viability and retention of the engrafted AD-MSCs and demonstrated a reduction in ventricular remodelling post MI.

To recreate the intrinsic hierarchy of tendons, Almeida *et al.* developed a biomimetic scaffold using PCL, CS and cellulose nanocrystals.<sup>79</sup> The substrate's surface stiffness was reduced by coating with tropoelastin (TROPO) *via* PDA cross-linking. *In vitro* testing with human adipose-derived stem cells revealed that TROPO coatings sustained the tenogenic commitment of stem cells, promoting faster cell elongation and enabled the autologous synthesis of a tendon-like ECM.

Although PLLA is a promising biodegradable polymer within cardiac research, it does have some disadvantages including high hydrophobicity and reduced cell adhesion. Bolbasov *et al.* modified the surface of PLLA with a thin titanium oxynitride (TiO<sub>x</sub>N<sub>y</sub>) / titanium nitride (TiN<sub>x</sub>) / TiO / TiO<sub>2</sub> mixed coating utilising reactive magnetron sputtering within a nitrogen atmosphere.<sup>80</sup> Various plasma treatment times were evaluated to reveal that physico-mechanical properties of the scaffold remained unchanged and hydrophobicity was decreased. No adverse tissue reaction was documented during *in vivo* subcutaneous implantation (Wistar rats) of the modified PLLA scaffolds up to 3 months and re-growth of replacement tissue was discerned to depend upon plasma treatment time.

Lee *et al.* developed a 'nature-inspired catechol-conjugated hyaluronic acid environment' coating platform (NiCHE) for enhancing the efficacy of salivary gland tissue.<sup>81</sup> The NiCHE coating (adhesive hyaluronic acid-catechol), dip-coated onto PCL scaffolds and polycarbonate, increased proliferation of vascular endothelial cells.

Although PLGA, PGA and PLA are widely utilised within the field of tissue engineering there are some disadvantages to their use, including inflammatory responses linked to the release of acidic products during degradation. To address this issue, Shen *et al.* detail the production of unidirectional shell-core structured fibres of CS/poly(lactide-co-glycolide) *via* coaxial electrospinning.<sup>82</sup> CS has an acid-neutralising capability, and the coatings established on the PLGA fibres slowed the pH decrease associated with degradation of PLGA *in vitro* as well as significantly reducing the production of inflammatory factors and down-regulating (reducing) the expression of related inflammatory genes (human dermal fibroblasts). Further biocompatibility assays showed the coated fibres to be biocompatible, *in vivo* testing (subcutaneous implantation) demonstrated that the CS coating decreased the recruitment of inflammatory cells and the formation of foreign body giant cells.

Landry *et al.* reveal the challenges associated with long-term primary neural cell culture including the juxtaposition of providing a surface that is not only soft and hydrophilic but also robust and bound strongly enough to the underlying surface to provide an adequate support for long-term cell growth.<sup>83</sup> To this end, the authors also reviewed recent developments of new artificial extracellular matrix (ECM) surfaces for *in vitro* neural cell culture.

Shrestha *et al.* utilised electrospinning to produce a self-electrical stimulated double-layered nerve guidance conduit creating a bioactive framework of CS-grafted PU integrated with functionalised multiwall carbon nanotubes and coated with PPy.<sup>84</sup> The structural framework exhibited biocompatibility; aligned orientated fibres showed accelerated regrowth, proliferation and migration of Schwann cells and differentiation of rat pheochromocytoma cells compared to randomly orientated mats exemplifying the potential of nerve guidance conduits for use in nerve tissue regeneration.

To address the issue of chronically implanted microelectrode array (MEA) isolation from the brain due to foreign body response, Cassar *et al.* developed an electrodeposited platinum-iridium coating for use with penetrating recording MEAs.<sup>85</sup> *In vivo* testing led to the conclusion that coated MEAs provided improved recording performance in comparison to uncoated arrays.

Yan *et al.* coated a silk fibroin sponge internally and externally with collagen (dip-coating followed by a crosslinking step) that was used to replace the meniscus (stabilising cartilage) of the knee removed during meniscectomy (removal of this cartilage).<sup>86</sup> The scaffold produced demonstrated that the collagen coating improved biocompatibility, frictional properties and tissue ingrowth of the sponge *in vivo*.

Recognising the need for bioactive composite scaffolds with favourable mechanical properties, Luo *et al.* utilised 3D-printing and *in-situ* mineralisation to produce alginate/gelatin scaffolds with a homogenous nano apatite coating; the coating thickness could be controlled by the phosphate ion concentration.<sup>87</sup> In comparison to uncoated scaffolds, the coated scaffold exhibited superior mechanical properties (2-fold higher Young's modulus), and accelerated proliferation and osteogenic differentiation of rat bone marrow cells.

### Biosensors

Methods used for depositing nanomaterials onto electrode surfaces to produce efficient biosensors have been reviewed by Ahmad *et al.*<sup>88</sup> These are grouped broadly into coatings,

direct deposition, printing and direct growth, which are further subdivided. Protein-resistant polymer coating strategies for biosensors and biomaterials have been reviewed and discussed by Zhang *et al.*<sup>89</sup> A review by Chen and Noy categorises the antifouling strategies to protect bioelectronic devices;<sup>90</sup> relevant to polymer coatings, self-polishing, temperature-responsive, pH-responsive, phospholipid coatings (that mimic cell membranes), PEGs, polymer brushes, and hydrogel coatings are described. Xu and Lee have also reviewed various strategies used to prolong the life of biosensors, particularly in the area of delaying biofouling through the use of various hydrophilic, biomimetic, drug-eluting, zwitterionic, and other smart polymer materials.<sup>91</sup> PEGs and zwitterionic polymers are considered 'gold standards' as coatings for reducing biofouling of biosensors, although Chan *et al.* reported success in using a polyacrylamide-based copolymer hydrogel for this application;<sup>92</sup> certain copolymer compositions showed better performance than the gold standards.

Burugapalli *et al.* used electrospun membranes of PU and gelatin to produce *in vivo* implantable glucose biosensors of high sensitivity.<sup>93</sup>

Liu *et al.* reported a PVP coating that protects MNs (vertical ZnO nanowires) for use in transdermal biosensing of H<sub>2</sub>O<sub>2</sub>.<sup>94</sup> PVP was spray-coated on to MN surface and offered a 3-fold protection over uncoated surfaces.

The entrapment of *Aspergillus niger* (a fungus) in ICPs, such as PPy, is an established method of producing amperometric glucose sensors.<sup>95</sup> Apetrei *et al.* found that the sensitivity of such biosensors was improved by forming PPy *in situ* with the cellular membrane/wall.<sup>95</sup>

## Conclusions

Polymer coatings are invaluable in the field of biomedical applications, due to their biocompatibility, functionality, durability and stability (chemical, biological and physical). Thus, these coatings find applications in orthopaedics, cardiovascular stents, antibacterial surfaces, drug delivery, tissue engineering and biosensors, among other lesser studied applications. Ceramic coatings are also of great interest, although the applications currently tend to be more focused in the area of orthopaedic implants.

## Disclosure statement

No potential conflict of interest was reported by the author(s).

## ORCID

J. R. Smith  <http://orcid.org/0000-0001-8805-3788>

D. A. Lamprou  <http://orcid.org/0000-0002-8740-1661>

S. J. Upson  <http://orcid.org/0000-0002-0428-5977>

## References

- H. Li, D. Huang, K. Ren and J. Ji: *Smart Mater. Med.*, **2021**, **2**, 1–14.
- J. R. Smith and D. A. Lamprou: *Trans. IMF.*, **2014**, **92**(1), 9–19.
- K. Alizadeh-Osgoue, Y. Li and C. Wen: *Bioactive Mater.*, **2019**, **4**, 22–36.
- D. Bhagya Mathi, D. Gopi and L. Kavitha: *Mater. Today: Proc.*, **2020**, **26**, 3526–3530.
- R. Mohan Raj, N. Duraisamy and V. Raj: *Mater. Today: Proc.*, *in press*. doi:10.1016/j.matpr.2020.10.772.
- E. Mahlooji, M. Atapour and S. Labbaf: *Carbohydrate Polym.*, **2019**, **226**, 115299.
- R. Mohan Raj, P. Priya and V. Raj: *J. Mech. Behav. Biomed. Mater.*, **2018**, **82**, 299–309.
- S. Kumari, H. R. Tiyyagura, Y. B. Pottathara, K. K. Sadasivuni, D. Ponnamma, T. E. L. Douglas, A. G. Skirtach and M. K. Mohan: *Carbohydrate Polym.*, **2021**, **255**, 117487.
- D. Gopi, A. Karthika, S. Nithiya and L. Kavitha: *Mater. Chem. Phys.*, **2014**, **144**, 75–85.
- S. Krishnakumar and T. Senthilvelan: *Mater. Today: Proc.*, **2021**, **46** (19), 9707–9713. doi:10.1016/j.matpr.2020.08.463.
- J. Pan, S. Prabakaran and M. Rajan: *Biomed. Pharm.*, **2019**, **119**, 109404.
- A. Abdal-hay, M. Agour, Y.-K. Kim, M.-H. Lee, M. K. Hassan, H. Abu El-Ainin, A. S. Hamdy and S. Ivanovski: *Eur. Polym. J.*, **2019**, **112**, 555–568.
- A. M. Kumar, A. Y. Adesina, M. A. Hussein, S. A. Umoren, S. Ramakrishna and S. Saravanan: *Carbohydrate Polym.*, **2020**, **242**, 116285.
- N. Shokri, M. S. Safavi, M. Etminanfar, F. C. Walsh and J. Khalil-Allafi: *Mater. Chem. Phys.*, **2021**, **259**, 124041.
- I. Mendolia, C. Zanca, F. Ganci, G. Conoscenti, F. Carfi Pavia, V. Brucato, V. La Carrubba, F. Lopresti, S. Piazza, C. Sunseri and R. Inguanta: *Surf. Coat. Technol.*, **2021**, **408**, 126771.
- M. Samiee, M. Hanachi, Z. S. Seyedraoufi, M. J. Eshraghi and Y. Shajari: *Ceramics Int.*, **2021**, **47**, 6179–6186.
- D. Alves, P. Borges, T. Grainha, C. F. Rodrigues and M. O. Pereira: *Mater. Sci. Eng. C.*, **2021**, **120**, 111742.
- L. Jia, F. Han, H. Wang, C. Zhu, Q. Guo, J. Li, Z. Zhao, Q. Zhang, X. Zhu and B. Li: *J. Orthopaedic Transl.*, **2019**, **17**, 82–95.
- E. J. Benjamin, S. S. Virani, C. W. Callaway, et al.: *Circulation*, **2018**, **137** (12), e67–e492.
- L. Navarro, G. Duffó, D. Vetcher, V. P. Moles, J. A. Luna and I. Rintoul: *Trends Med.*, **2020**, **20**, doi:10.15761/TIM.1000220.
- S. Borhani, S. Hassanajili, S. H. A. Tafti and S. Rabbani: *Progr. Biomaterials*, **2018**, **7**, 175–205.
- N. Beshchasna, M. Saqib, H. Kraskiewicz, Ł. Wasyluk, O. Kuzmin, O. C. Duta, D. Fica, Z. Ghizdave, A. Marin, A. Fica, Z. Sun, V. F. Pichugin, J. Opitz and E. Andronescu: *Pharmaceutics*, **2020**, **12**(4), 349, doi:10.3390/pharmaceutics12040349.
- M. Livingston and A. Aaron Tan: *J. Med. Device.*, **2019**, **10**(1). doi:10.1115/1.4031718.
- D.-H. Lee and J. M. de la Torre Hernandez: *Eur. Cardiol. Rev.*, **2018**, **13** (1), 54–59. doi:10.15420/ocr.2018.8:2.
- S. Torii, H. Jinnouchi, A. Sakamoto, M. Kutyna, A. Cornelissen, S. Kuntz, L. Guo, H. Mori, E. Harari, K. H. Paek, R. Fernandez, D. Chahal, M. E. Romero, F. D. Kolodgie, A. Gupta, R. Virmani and A. V. Finn: *Nature Reviews Cardiology*, **2020**, **17**, 37–51.
- I. Rykowska, I. Nowak and R. Nowak: *Molecules*, **2020**, **25**, 4624. doi:10.3390/molecules25204624.
- J. Nogic, L. M. McCormick, R. Francis, N. Nerlekar, C. Jaworski, N. E. J. West and A. J. Brown: *J. Cardiol.*, **2018**, **71**, 435–443.
- T. Qiu and L. Zhao: *Vessel Plus*, **2018**, **2**, 12. C10. doi:10.20517/2574-1209.2018.13.
- F. Krackhardt, V. Kočka, M. W. Waliszewski, A. Utech, M. Lustermann, M. Hudec, M. Studenčan, M. Schwefer, J. Yu, M. H. Jeong, T. Ahn, W. A. W. Ahmad, M. Boxberger, A. Schneider and M. Leschke: *Open Heart*, **2017**, **4**, e000592. doi:10.1136/openhrt-2017-000592.
- C. M. McKittrick, M. J. Cardona, R. A. Black and C. M. McCormick: *Ann. Biomed. Eng.*, **2020**, **48**(1), 271–281. doi:10.1007/s10439-019-02346-6.
- R. V. Jeger, A. Farah, M.-A. Ohlow, N. Mangner, S. Möbius-Winkler, D. Weilenmann, J. Wöhrle, G. Stachel, S. Markovic, G. Leibundgut, P. Rickenbacher, S. Osswald, M. Cattaneo, N. Gilgen, C. Kaiser and B. Scheller: *Lancet*, **2020**, **396**, 1504–1510.
- V. Bakola, V. Karagkiozaki, A. R. Tsiapla, F. Pappa, I. Moutsios, E. Pavlidou and S. Logothetidis: *Nanotechnology*, **2018**, **29**, 275101.
- I.-H. Bae, M. H. Jeong, D. S. Park, K. S. Lim, J. W. Shim, M. K. Kim and J.-K. Park: *Biomater. Res.*, **2020**, **24**, 4. doi:10.1186/s40824-020-0182-x.
- P. Roopmani, S. Satheesh, D. C. Raj and U. M. Krishnan: *ACS Biomater. Sci. Eng.*, **2019**, **5**, 2899–2915.
- J. Liu, J. Wang, Y.-f. Xue, T.-t. Chen, D.-n. Huang, Y.-x. Wang, K.-f. Ren, Y.-b. Wang, G.-s. Fu and S. Ji: *J. Mater. Chem. B*, **2020**, **8**, 5361–5368.
- Y. Yang, P. Gao, J. Wang, Q. Tu, L. Bai, K. Xiong, H. Qiu, X. Zhao, M. F. Maitz, H. Wang, X. Li, Q. Zhao, Y. Xiao, N. Huang and Z. Yang: *AAAS Res.*, **2020**, 9203906. doi:10.34133/2020/9203906.
- X. Li, H. Qiu, P. Gao, Y. Yang, Z. Yang and N. Huang: *NPG Asia Mater.*, **2018**, **10**, 482–496. doi:10.1038/s41427-018-0052-3.

38. G. A. Lakalayeh, M. Rahvar, E. Haririan, R. Karimi and H. Ghanbari: *Artificial Cells Nanomed. Biotechnol.*, **2018**, **46**(7), 1380–1389. doi:10.1080/21691401.2017.1369424.
39. W. Xu, K. Yagoshi, T. Asakura, M. Sasaki and T. Niidome: *ACS Appl. Bio. Mater.*, **2020**, **3**, 531–538.
40. W. Xu, K. Yagoshi, Y. Koga, M. Sasaki and T. Niidome: *Colloids Surf. B Biointerfaces*, **2018**, **163**, 100–106.
41. L. Chen, J. Li, S. Wang, S. Zhu, C. Zhu, B. Zheng, G. Yang and S. Guan: *J. Mater. Res.*, **33**(23), 4123–4133.
42. Z. Huang and H. Ghasemi: *Adv. Colloid Interf. Sci.*, **2020**, **284**, 102274.
43. O. Bazaka, K. Bazaka, V. K. Truong, I. Levchenko, M. V. Jacob, Y. Estrin, R. Lapovok, B. Chichkov, E. Fadeeva, P. Kingshott, R. J. Crawford and E. P. Ivanova: *Appl. Surf. Sci.*, **2020**, **521**, 146375.
44. A. Valliammai, A. Selvaraj, P. Mathumitha, C. Aravindraj and S. K. Pandian: *Mater. Sci. Eng. C.*, **2021**, **121**, 111863.
45. L. L. Guo, Y. F. Chen, X. Ren, K. Gopinath, Z. S. Lu, C. M. Li and L. Q. Xu: *Colloids Surf. B: Biointerfaces*, **2021**, **200**, 111592.
46. L. Liu, W. Peng, X. Zhang, J. Peng, P. Liu and J. Shen: *J. Mater. Sci. Technol.*, **2021**, **62**, 96–106.
47. M. Czuban, M. W. Kulka, L. Wang, A. Koliszak, K. Achazi, C. Schlaich, I. S. Donskyi, M. D. Luca, J. M. M. Oneto, M. Royzen, R. Haag and A. Trampuz: *Mater. Sci. Eng. C.*, **2020**, **116**, 111109.
48. S. Dhingra, A. Joshi, N. Singh and S. Saha: *Mater. Sci. Eng. C.*, **2021**, **118**, 111465.
49. L. Valencia, S. Kumar, B. Jalvo, A. Mautner, G. Salazar-Alvarez and A. P. Mathew: *J. Mater. Chem. A*, **2018**, **6**(34), 16361–16370.
50. X. Wang, X. Li, X. Yang, K. Lei and L. Wang: *Colloids Surf. B: Biointerfaces*, **2021**, **197**, 111410.
51. Z. Li, S. Wang, X. Yang, H. Liu, Y. Shan, X. Xu, S. Shang and Z. Song: *Appl. Surf. Sci.*, **2020**, **530**, 147193.
52. J. L. Low, P. H.-N. Kao, P. A. Tambyah, G. L. E. Koh, H. Ling, K. A. Kline, W. S. Cheow and S. S. J. Leong: *Biotechnol. Notes*, **2021**, **2**, 1–10.
53. Y.-T. Hung, L. A. McLandsborough, J. M. Goddard and L. J. Bastarrachea: *LWT Food Sci. Technol.*, **2018**, **97**, 546–554.
54. J. Su, J. Noro, S. Silva, J. Fu, Q. Wang, A. Rubeiro, C. Silva and A. Cavaco-Paulo: *Reactive Funct. Polym.*, **2019**, **136**, 25–33.
55. Y. Ahmadi and S. Ahmad: *Progr. Org. Coat.*, **2019**, **127**, 168–180.
56. D. H. K. Nguyen, O. Bazaka, K. Bazaka, R. J. Crawford and E. P. Ivanova: *Trends Bioechnol.*, **2020**, **38**(5), 558–571.
57. T. Saeedi, H. F. Alotaibi and P. Prokopovich: *Adv. Colloid Interface Sci.*, **2020**, **285**, 102273.
58. P. Jana, M. Shyam, S. Singh, V. Jayaprakash and A. Dev: *Eur. Polym. J.*, **2021**, **142**, 110155.
59. K. Khurana, F. Müller, K. Jacobs, T. Faidt, J.-U. Neurohr, S. Grandthyll, F. Mücklich, C. Canal and M. P. Ginebra: *Eur. Polym. J.*, **2018**, **107**, 25–33.
60. H. Yu, H. Tan, Y. Huang, J. Pan, J. Yao, M. Liang, J. Yang and H. Jia: *Biochem. Biophys. Res. Commun.*, **2020**, **526**(2), 328–333.
61. M. A. Sevostyanov, A. S. Baikin, K. V. Sergienko, L. A. Shatova, A. A. Kirsankin, I. V. Baymler, A. V. Shkirin and S. V. Gudkov: *React. Funct. Polym.*, **2020**, **150**, 104550.
62. Z. Y. Al Subeh, N.-Q. Chu, J. T. Korunes-Miller, L. L. Tsai, T. N. Graf, Y. P. Hung, C. J. Pearce, M. W. Grinstaff, A. H. Colby, Y. L. Colson and N. H. Oberlies: *J. Control. Release*, **2021**, **331**, 260–269.
63. E. Moghimipour, F. A. Dorkoosh, M. Rezaei, M. Kouchak, J. Fatahiasl, K. A. Angali, Z. Ramezani, M. Amini and S. Handali: *J. Drug Delivery Sci. Technol.*, **2018**, **43**, 50–56.
64. S. F. Barakh Ali, H. Afrooz, R. Hampel, E. M. Mohamed, R. Bhattacharya, P. Cook, M. A. Khan and Z. Rahman: *Int. J. Pharm.*, **2019**, **567**, 118462.
65. P. McCrorie, J. Mistry, V. Taresco, T. Lovato, M. Fay, I. Ward, A. A. Ritchie, P. A. Clarke, S. J. Smith, M. Marlow and R. Rahman: *Eur. J. Pharm. Biopharm.*, **2020**, **157**, 108–120.
66. A. S. Rzhavskiy, T. R. R. Singh, R. F. Donnelly and Y. G. Anissimov: *J. Control. Release*, **2018**, **270**, 184–202.
67. P. Singh, A. Carrier, Y. Chen, S. Lin, J. Wang, S. Cui and X. Zhang: *J. Control. Release*, **2019**, **315**, 97–113.
68. Á Cárcamo-Martínez, Q. K. Anjani, A. D. Permana, A. S. Cordeiro, E. Larrañeta and R. F. Donnelly: *Int. J. Pharm. X*, **2020**, **2**, 100048.
69. X. Xu, S. Lü, C. Wu, Z. Wang, C. Feng, N. Wen, M. Liu, X. Zhang, Z. Liu, Y. Liu and C. Ren: *Microporous Mesoporous Mater.*, **2018**, **271**, 234–242.
70. S. Shidfar, F. Tavangarian, N. H. Nemati and A. Fahami: *Mater. Discovery*, **2017**, **8**, 9–17.
71. S. Peng, B. Ouyang, Y. Men, Y. Du, Y. Cao, R. Xie, Z. Pang, S. Shen and W. Yang: *Biomaterials*, **2020**, **231**, 119680.
72. A. Puiggalí-Jou, L. J. del Valle and C. Alemán: *J. Control. Release*, **2019**, **309**, 244–264.
73. M. Bansal, A. Dravid, Z. Aqrawe, J. Montgomery, Z. Wu and D. Svirskis: *J. Control. Release*, **2020**, **328**, 192–209.
74. S. Caddeo, M. Mattioli-Belmonte, C. Cassino, N. Barbani, M. Dicarolo, P. Gentile, F. Baino, S. Sartori, C. Vitale-Brovarone and G. Ciardelli: *Mater. Sci. Eng. C*, **2019**, **96**, 218–233.
75. A. Sandeep Kranthi Kiran, T. S. Sampath Kumar, R. Sanghavi, M. Doble and S. Ramakrishna: *Nanomaterials*, **2018**, **8**, 860. doi:10.3390/nano8100860.
76. N. Marival, M. Morenc, M. N. Labour, A. Samotus, A. Mzyk, V. Ollivier, M. Maire, K. Jesse, K. Bassand, A. Niemiec-Cyganek, O. Haddad, M. P. Jacob, F. Chaubet, N. Charnaux, P. Wilczek and H. Hlawaty: *Biomaterials*, **2018**, **172**, 14–29.
77. M. Iijima, H. Aubin, M. Steinbrink, F. Schiffer, A. Assmann, R. D. Weisel, Y. Matsui, R.-K. Li, A. Lichtenberg and P. Akhyari: *J. Tissue Eng. Regen. Med.*, **2018**, **12**, e513–e522.
78. J. Chen, Y. Zhan, Y. Wang, D. Han, B. Tao, Z. Luo, S. Ma, Q. Wang, X. Li, L. Fan, C. Li, H. Deng and F. Cao: *Acta Biomater.*, **2018**, **80**, 154–168.
79. H. Almeida, R. M. A. Domingues, S. M. Mithieux, R. A. Pires, A. I. Gonçalves, M. Gómez-Florit, R. L. Reis, A. S. Weiss and M. E. Gomes: *ACS Appl. Mater. Interfaces*, **2019**, **11**(22), 19830–19840. doi:10.1021/acsami.9b04616.
80. E. N. Bolbasov, P. V. Maryin, K. S. Stankevich, A. I. Kozelskaya, E. V. Shesterikov, Y. I. Khodyrevskaya, M. V. Nasonov, D. K. Shishkov, Y. A. Kudryavtsev, Y. G. Anissimov and S. I. Tverdokhlebov: *Coll. Surf. B: Biointerfaces*, **2018**, **162**, 43–51.
81. S.-w. Lee, J. H. Ryu, M. J. Do, E. Namkoong, H. Lee and P. Park: *ACS Appl. Mater. Interfaces*, **2020**, **12**, 4285–4294.
82. Y. Shen, T. Tu, B. Yi, X. Wang, H. Tang, W. Liu and Y. Zhang: *Acta Biomater.*, **2019**, **97**, 200–215.
83. M. J. Landry, F.-G. Rollet, T. E. Kennedy and C. J. Barrett: *Langmuir*, **2018**, **34**, 8709–8730.
84. S. Shrestha, B. K. Shrestha, J. I. Kim, S. W. Ko, C. H. Park and C. S. Kim: *Carbon*, **2018**, **136**, 430–443.
85. I. R. Cassar, C. Yu, J. Sambangi, C. D. Lee, J. J. Whalen III, A. Petrossians and W. M. Grilla: *Biomaterials*, **2019**, **205**, 120–132.
86. R. Yan, Y. Chen, Y. Gu, C. Tang, J. Huang, Y. Hu, Z. Zheng, J. Ran, B. Heng, X. Chen, Z. Yin, W. Chen, W. Shen and H. Ouyana: *J. Tissue Eng. Regen. Med.*, **2019**, **13**, 156–173.
87. Y. Luo, Y. Li, X. Qin and Q. Wa: *Mater. Design*, **2018**, **146**, 12–19.
88. R. Ahmad, O. S. Wolfbeis, Y.-B. Hahn, H. N. Alshareef, L. Torsi and K. N. Salama: *Mater. Today Commun.*, **2018**, **17**, 289–321.
89. T.-D. Zhang, X. Zhang and X. Deng: *Ann. Biotechnol.*, **2018**, **2**, 1006.
90. X. Chen and A. Noy: *APL Mater.*, **2021**, **9**, 020701. doi:10.1063/5.0029994.
91. J. Xu and H. Lee: *Chemosensors*, **2020**, **8**, 66. doi:10.3390/chemosensors8030066.
92. D. Chan, J.-C. Chien, E. Axpe, L. Blankemeier, S. W. Baker, S. Swaminathan, V. A. Piunova, D. Y. Zubarev, H. T. Soh and E. A. Appel: *bioRxiv*, 0. doi:10.1101/2020.05.25.115675.
93. K. Burugapalli, S. Wijesuriya, N. Wang and W. Song: *J. Biomed. Mater. Res. Part A.*, **2018**, **106A**, 1072–1081.
94. F. Liu, Z. Lin, Q. Jin, Q. Wu, C. Yang, H.-J. Chen, Z. Cao, D.-a. Lin, L. Zhou, T. Hang, G. He, Y. Xu, W. Xia, J. Tao and X. Xie: *ACS Appl. Mater. Interfac.*, **2019**, **11**(5), 4809–4819. doi:10.1021/acsami.8b18981.
95. R.-M. Apetrei, G. Cârâc, G. Bahrim and P. Camurlu: *Int. J. Polym. Mater. Polym. Biomater.*, **2018**, **68**(17), 1058–1067.